

ORIGINAL ARTICLE

High coverage metabolomics analysis reveals phage-specific alterations to *Pseudomonas aeruginosa* physiology during infection

Jeroen De Smet¹, Michael Zimmermann², Maria Kogadeeva², Pieter-Jan Ceysens^{1,3}, Wesley Vermaelen¹, Bob Blasdel¹, Ho Bin Jang¹, Uwe Sauer² and Rob Lavigne¹

¹Laboratory of Gene Technology, Department of Biosystems, KU Leuven, Heverlee, Belgium; ²Institute of Molecular Systems Biology, Eidgenössische Technische Hochschule (ETH) Zürich, Zürich, Switzerland and

³Unit Bacterial Diseases, Scientific Institute of Public Health (WIV-ISP), Brussels, Belgium

Phage-mediated metabolic changes in bacteria are hypothesized to markedly alter global nutrient and biogeochemical cycles. Despite their theoretic importance, experimental data on the net metabolic impact of phage infection on the bacterial metabolism remains scarce. In this study, we tracked the dynamics of intracellular metabolites using untargeted high coverage metabolomics in *Pseudomonas aeruginosa* cells infected with lytic bacteriophages from six distinct phage genera. Analysis of the metabolomics data indicates an active interference in the host metabolism. In general, phages elicit an increase in pyrimidine and nucleotide sugar metabolism. Furthermore, clear phage-specific and infection stage-specific responses are observed, ranging from extreme metabolite depletion (for example, phage YuA) to complete reorganization of the metabolism (for example, phage phiKZ). As expected, pathways targeted by the phage-encoded auxiliary metabolic genes (AMGs) were enriched among the metabolites changing during infection. The effect on pyrimidine metabolism of phages encoding AMGs capable of host genome degradation (for example, YuA and LUZ19) was distinct from those lacking nuclease-encoding genes (for example, phiKZ), which demonstrates the link between the encoded set of AMGs of a phage and its impact on host physiology. However, a large fraction of the profound effect on host metabolism could not be attributed to the phage-encoded AMGs. We suggest a potentially crucial role for small, ‘non-enzymatic’ peptides in metabolism take-over and hypothesize on potential biotechnical applications for such peptides. The highly phage-specific nature of the metabolic impact emphasizes the potential importance of the ‘phage diversity’ parameter when studying metabolic interactions in complex communities.

The ISME Journal (2016) 10, 1823–1835; doi:10.1038/ismej.2016.3; published online 16 February 2016

Introduction

Ever since Bergh *et al.* (1989) published the numeric abundance of viruses in aquatic environments, viruses have been predicted to cause large fluctuations in global nutrient and biogeochemical cycles (Suttle, 2005; Danovaro *et al.*, 2008; Falkowski *et al.*, 2008). These global effects are primarily caused by microbial mortality following infection, which impacts microbial abundance and diversity (Suttle, 2005). As viruses are deprived of an own metabolism, they have to exploit their host cells’ resources to fuel viral replication during infection. To overcome possible bottlenecks in this process, many virus genomes have acquired host-derived genes with metabolic functions, which

are hypothesized to reprogram the host’s metabolic processes to favor virus replication and are termed ‘auxiliary metabolic genes’ (AMGs) (Breitbart *et al.*, 2007). The increased availability of metagenomic sequencing data over the past decade enabled identification of many AMGs in eukaryotic and prokaryotic viruses, with intervening roles in phosphate (Martiny *et al.*, 2009) and nitrogen metabolism (Sullivan *et al.*, 2010), photosynthesis (Lindell *et al.*, 2005; Frank *et al.*, 2013), the pentose phosphate pathway (Thompson *et al.*, 2011), nucleic acid synthesis (Miller *et al.*, 2003) and other metabolic pathways (Sharon *et al.*, 2011). Currently, AMGs are known to be spread across nearly the entire central carbon metabolism (Hurwitz *et al.*, 2013). In an attempt to organize the expanding list of AMGs, Hurwitz *et al.* (2015) proposed a subdivision into two classes. Class I contains annotations present in KEGG metabolic pathways, whereas Class II are all genes annotated only with a general metabolic function or absent from KEGG metabolic pathways (for example, transport functions).

Correspondence: R Lavigne, Laboratory of Gene Technology, Department of Biosystems, KU Leuven Kasteelpark Arenberg 21, Heverlee 3001, Belgium.

E-mail: Rob.Lavigne@kuleuven.be

Received 15 June 2015; revised 26 November 2015; accepted 16 December 2015; published online 16 February 2016

Another feature of viral genomes is the high number of encoded open reading frames with no similarity to any known sequence (approximately 60% in marine viruses) (Paul and Sullivan, 2005), often referred to as the biological ‘dark matter’ (Rohwer and Youle, 2011). Especially early in infection, these small gene products of unknown function can influence the host metabolism through specific, often uncharacterized interactions, which are impossible to predict (Hatfull, 2008; Roucourt and Lavigne, 2009; Hargreaves *et al.*, 2014). The identification of such viral–host interactions, and the viral genes involved, has proven to be labor-intensive research. However, recent advances in -omics techniques provide us with the tools to obtain novel insights into the host take-over process and to identify the affected host metabolic pathways (Van den Bossche *et al.*, 2014; Sanchez *et al.*, 2015).

In contrast to the increasing knowledge concerning the genetic potential of phages for host metabolism take-over, experimental data on the host metabolic changes caused by the phage infection and the influence of encoded AMGs on these changes are extremely scarce. Current advances in the field of metabolomics, triggered by the progress in mass spectrometry (Rabinowitz, 2007), allow analysis of multiple time points during infection with high metabolite coverage (Timischl *et al.*, 2008). Ankrah *et al.* (2014) were the first to apply these approaches to investigate the phage infection of an environmentally relevant bacterium. Their results showed significant physiological differences between phage-infected and non-infected cells and raised the question if this response could be generalized to different phage–host systems. Furthermore, metabolomics has proven to be a valuable tool in functional genomics to characterize unknown proteins (Ehebauer *et al.*, 2015). As enzyme inactivation leads to upstream accumulation of metabolites (Fendt *et al.*, 2010), whereas protein activity modulation through post-translational modification or protein interaction also impacts metabolism (Oliveira *et al.*, 2012; Schulz *et al.*, 2014).

In this study, we selected the ubiquitous, Gram-negative bacterial pathogen, *Pseudomonas aeruginosa*, as a host system to investigate the phage–host metabolome interaction. This bacterium has an extreme metabolic versatility, allowing it to survive

in diverse habitats ranging from coastal marine habitats over soil to even human tissue, making it an ideal model organism (Stover *et al.*, 2000). Using flow injection analysis time-of-flight mass spectrometry (Fuhrer *et al.*, 2011), we studied the metabolite dynamics in *P. aeruginosa*, during different stages of infection by diverse well-characterized lytic double-stranded DNA phages (Table 1, Ceyssens and Lavigne, 2010). The goal was to determine if phage infection results in a metabolic, ‘universal’ host response or if different phage species will yield distinguishable responses, a question that, to our knowledge, has never been addressed to date.

Materials and methods

P. aeruginosa strain and phage isolates

P. aeruginosa strain PAO1 (genotype 0002) was chosen as bacterial host system in view of its extensive genetic and phenotypic characterization. First isolated in 1955 in Melbourne, Australia from an infected wound (Holloway, 1955), it was the first fully sequenced *P. aeruginosa* strain (Stover *et al.*, 2000). Six different lytic phages were selected to represent a diverse set of *Pseudomonas* bacteriophages (Table 1). Phage stocks were grown on their original *P. aeruginosa* propagation strain, that is, PAO1 (LUZ19, PEV2, 14-1, YuA and phiKZ) or Li010 (LUZ24) using standard soft agar overlay followed by PEG8000 precipitation, as previously described (Ceyssens *et al.*, 2008), and stored in phage buffer (10 mM Tris-HCl, pH 7.5, 10 mM MgSO₄, 150 mM NaCl) at 4 °C.

Construction of the virus population network

To illustrate the genome-based relationship between the selected phages, the predicted protein sequences representing the genomes of LUZ24, LUZ19, 14-1, PEV2, phiKZ and YuA, as well as their potentially relevant bacteriophages were clustered using the ACLAME database, version 0.4 (<http://aclame.ulb.ac.be>) with the database of ‘Viruses’ and E-value cutoff of 0.001 and all-to-all BLASTp searches with a cutoff E-value of 10⁻⁴ (Leplae *et al.*, 2004). The degree of similarity between phages was calculated as the minus logarithmic score by multiplying

Table 1 Main characteristics of the phages used in this study

Phage	Family	Genus	Genome (bp)	# ORFs	GC %	Infection cycle	Start viral replication	Burst size (# particles)	Reference
LUZ19	Podoviridae	Phikmvlikevirus	43 548	54	62.2	24 min	14 min	ND	Lammens <i>et al.</i> , 2009
LUZ24	Podoviridae	Luz24likevirus	45 625	68	52	45 min	ND	60	Ceyssens <i>et al.</i> , 2008
PEV2	Podoviridae	N4likevirus	72 543	90	54.9	35 min	ND	60	Ceyssens <i>et al.</i> , 2010
14-1	Myoviridae	Phunlikevirus	66 238	90	55.6	15 min	ND	ND	Ceyssens <i>et al.</i> , 2009
phiKZ	Myoviridae	Phikzlikevirus	280 334	306	36	60–65 min	ND	ND	Mesyanzhinov <i>et al.</i> , 2002
YuA	Siphoviridae	YuAlikevirus	58 663	78	64.3	80 min	ND	ND	Ceyssens <i>et al.</i> , 2008

Abbreviations: GC, genomic GC content; ND, not determined; ORF, open reading frame.

hypergeometric similarity *P*-value by the total number of pairwise comparisons. Afterward, a protein-sharing network was generated with the Cytoscape software platform, version 3.1.1, using an edge-weighted spring embedded model (Shannon *et al.*, 2003).

Medium and infection parameters characterization

All growth experiments were performed in minimal medium *Pseudomonas* (30 mM Na₂HPO₄, 14 mM KH₂PO₄, 20 mM (NH₄)₂SO₄, 20 mM glucose, 1 mM MgSO₄, 4 μM FeSO₄). Infection curves were determined by following the OD_{600nm} of a bacterial culture (OD_{600nm} = 0.3) every 5 min during infection until cell lysis was observed. Different multiplicity of infection (MOI) were used for all phages to ensure synchronized bacterial cell lysis and the optimal MOI was chosen (data not shown). Owing to differences in adsorption efficiency, the selected MOI varies between phages (Supplementary Figure S1). As the excess of phages is removed during the metabolome extraction, these differences will not impact the comparison between phages. During sampling, infection curves were made to assure infection of the entire culture (Supplementary Figure S1).

To check the efficiency of infection, cell counts of the infected culture were done before and 5 min after infection for all sampling and the obtained cell counts were compared. The efficiency of infection was >95% for phiKZ and 14-1, >90% for LUZ19 and YuA, >75% for PEV2 and >65% for LUZ24. Although there are differences in the efficiency of infection, they do not affect the comparison of metabolic alterations induced by the phages. As increasing the MOI did not affect the efficiency of infection, nor did it alter the infection curves, which show a synchronous infection (Supplementary Figure S1).

Metabolite extraction and analysis

Bacteria, grown in 75 ml of minimal medium *Pseudomonas*, were infected with phages at OD₆₀₀ = 0.3 (1.25 × 10⁸ CFU ml⁻¹) and sampled for metabolite profiling by fast filtration (Link *et al.*, 2013) at different time points during phage infection (Supplementary Figure S1). At each time point, the biomass quantity was measured by following the OD₆₀₀ and the sampling volumes were adjusted to a volume corresponding to a biomass of a 1 ml culture at OD₆₀₀ = 1.0 (approximately 4 × 10⁸ CFU). The samples were vacuum filtered through a 0.45 μm pore size nitrocellulose filter (Millipore, Billerica, MA, USA) and washed with 2 ml ammonium carbonate solution (75 mM, pH 7.0). The filters containing the captured cells were incubated in 3 ml ethanol (60%) at 78 °C for 2 min, and subsequently snap frozen in liquid nitrogen and stored at -80 °C until further processing. Metabolite extracts were dried at 30 °C under vacuum and re-suspended in 100 μl water. The samples were profiled using negative mode flow injection-time-of-flight mass spectrometry and detected ions were annotated as previously

reported (Fuhrer *et al.*, 2011). For each phage infection, four biological replicates were sampled and two technical repeats were made of each independent biological sample.

Metabolite data analysis

A genome-scale metabolic model of *P. aeruginosa* (Oberhardt *et al.*, 2008) and KEGG database were used to compile a metabolite reference list, according to which ions were assigned to metabolites applying a mass tolerance of 1 mDa and an intensity cutoff of 1500 counts. For each ion, only the metabolites with the highest annotation score were used, and for each metabolite, the best annotation was kept. Metabolite annotation and statistical analysis was performed using Matlab R2013b (Mathworks, Natick, MA, USA). A detailed description of these statistical analyses can be found in the Supplemental Materials and methods.

Results and Discussion

The selected Pseudomonas phages are highly diverse representatives within a broad virus population network

To investigate the occurrence of phage-specific effects on host metabolism, we aimed at selecting phages with possibly diverse infection phenotypes. To illustrate this, we constructed a virus population network, which includes the known (lytic) *Pseudomonas* phages, based on protein sequence similarities using the ACLAME database. The selected phages: LUZ19, LUZ24, PEV2, 14-1, phiKZ and YuA represent different branches within this network (Figure 1). Phages PEV2 and phiKZ are restricted to two components corresponding to the N4- and phiKZ-related groups, respectively; separated from the largest connected component. These individual components, attributable to their distinct shared core proteins, support the taxonomic descriptions as evolutionary distinct branches. In addition, phages LUZ24, 14-1 and LUZ19 fall into interconnected regions comprising the 7 LUZ24-like phages, 13 PB1-like phages and 3 phiKMV-like phages within the *Autographivirinae* clade, respectively. Each region contains one or more phage groups, implying their close evolutionary relationships. YuA shares proteins with multiple groups, with M6 as its closest relative. Collectively, as these phages belong to individual genera, the six studied phages provide an important basis for the understanding of the diversity of *Pseudomonas* phages in various viral lineages. Table 1 further illustrates that these phages differ strongly in genome size, GC-content and the duration of their infection cycle.

Phage infection disrupts the metabolic steady state in exponentially growing cells

To investigate the dynamic response of the host metabolism to infection with different phages, we

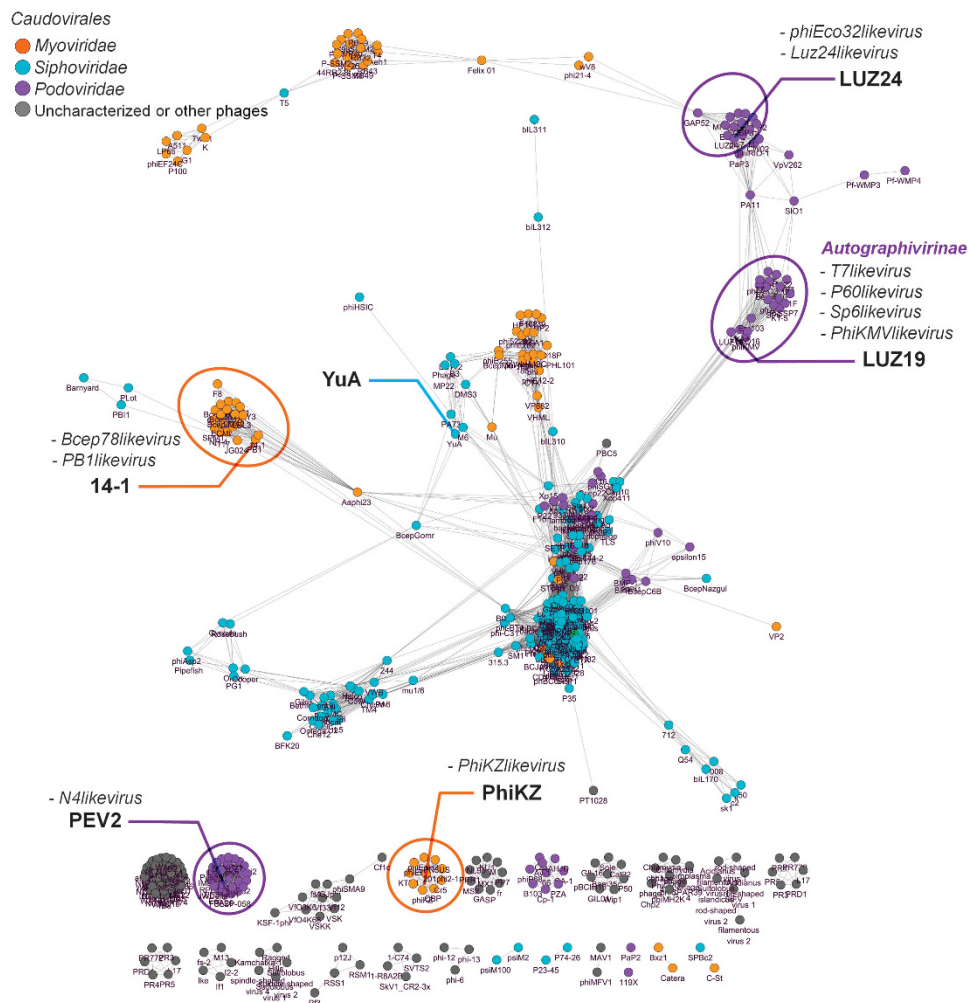


Figure 1 Virus population network reveals distinct clusters within the *Pseudomonas* phage universe. The network consists of 498 phages belonging to the *Myoviridae*, *Siphoviridae*, *Podoviridae*, or uncharacterized and other phages, and 6953 relationships between them. The nodes in the network are linked by edges indicating the significant relationships between viruses, in terms of shared gene (protein) contents. The viruses with a stringency similarity score of ≥ 1 , which is estimated using the hypergeometric formula, are shown. The network was visualized with an edge-weighted spring embedded layout using Cytoscape software platform (version 3.1.1), which places the viral genomes sharing more protein families closer in the display. Selected phages are shown in circle and named in bold. Orange = *Myoviridae*, teal = *Siphoviridae*, purple = *Podoviridae*, gray = uncharacterized.

performed a time-course experiment, infecting *P. aeruginosa* with each of the six selected phages and sampling the metabolic content at different stages of infection. To ensure synchronized infection and sample uniformity during the experiment, the MOI was adjusted and killing curves were made for individual phages to confirm synchronized infection (Supplementary Figure S1, Materials and methods). Samples were analyzed with untargeted flow injection analysis time-of-flight mass spectrometry, which allowed high coverage measurements of the metabolome. A total of 6006 ions were detected, of which 918 could be assigned to *P. aeruginosa* metabolites. After stringent filtering of ion adducts, 375 unique ions corresponding to 518 metabolites, including mass isomers, were retained.

To compare the metabolite dynamics, metabolite fold changes were determined for each time point

relative to time point zero of each infection. Without infection, metabolite levels remained stable, indeed only a small fraction of metabolites (3.2%) showed a (slight) increase after 45 min ($\log_2(\text{fold change}) < 0.5$) (Figure 2a). Compared with the metabolic steady-state of the non-infected samples, phage infection was found to induce significant alterations (P -value ≤ 0.05 and $\text{abs}(\log_2(\text{fold change})) > 0.5$) in up to 24.5% of the detected metabolites, as the sum of increased (19.7%) and decreased (4.8%) metabolites (PEV2, 25 min after infection, Figure 2a). This is consistent with the results observed for the lytic roseophage ($\Phi 2047B$) infection in *Sulfitobacter* sp. 2047, where approximately 25% of the 82 measured metabolites were altered after a single infection cycle (60–120 min; Ankrah *et al.*, 2014), confirming that host physiology is significantly altered upon phage infection in different host systems.

A ‘universal’ metabolic host response to Pseudomonas phage infection does not occur

To identify potentially common metabolic responses to phage infection, changes in all annotated metabolites were compared among the different phages. In total, 56% of the metabolites were significantly altered by at least one phage (P -value < 0.05 and $\text{abs}(\log_2(\text{fold change})) > 0.5$). However, only 2.4% of the metabolites were changed upon infection with each of the six phages, indicating the absence of a general response to phage infection (Figure 2b). In contrast, 17.30% of the metabolites were found to be significantly increased/decreased by a single phage, whereas staying stable in all others (Figure 2b, Supplementary Table S1).

The small percentage of changing metabolites (2.4%, nine metabolites) shared between all phages are involved in nucleotide and nucleotide sugar metabolism (Supplementary Table S2). Nucleotide metabolism produces the required nucleotides for viral genome replication, which was shown to be crucial during T7 infection (Qimron *et al.*, 2006). UDP-glucose and UDP-galactose are key intermediates for the production of oligo- and polysaccharides (Bosco *et al.*, 2009; Ebrecht *et al.*, 2015). For example, the nucleotide sugars (UDP-glucose, UDP-alpha-D-ManNAc3NAcA and UDP-alpha-D-GlcNAc3NAcA)

are precursors for lipopolysaccharide biosynthesis (Westman *et al.*, 2009).

Hierarchical clustering of the metabolites and phages based on the metabolite fold changes relative to the uninfected state confirms the absence of a ‘universal’ host response (Figure 3). For each phage, the time point responses form a closely related cluster branch, and the metabolite groups that attribute to the branch separation are shown on the top of the figure and will be discussed in later paragraphs.

A comparative pathway analysis between phages reveals a central role for pyrimidine metabolism and accumulation of nucleotide/amino sugars

To assess whether specific metabolic pathways are targeted during phage infection, metabolite set enrichment analysis was performed to identify pathways enriched for accumulated or depleted metabolites. All significantly affected pathways have been summarized in Supplementary Figure S2. Aside from a gradual change over time in pathways involved in nucleotide and amino-acid metabolism (for example, PEV2), only limited temporal variation was found for the different phages. To facilitate visual comparison between phages, the enrichment

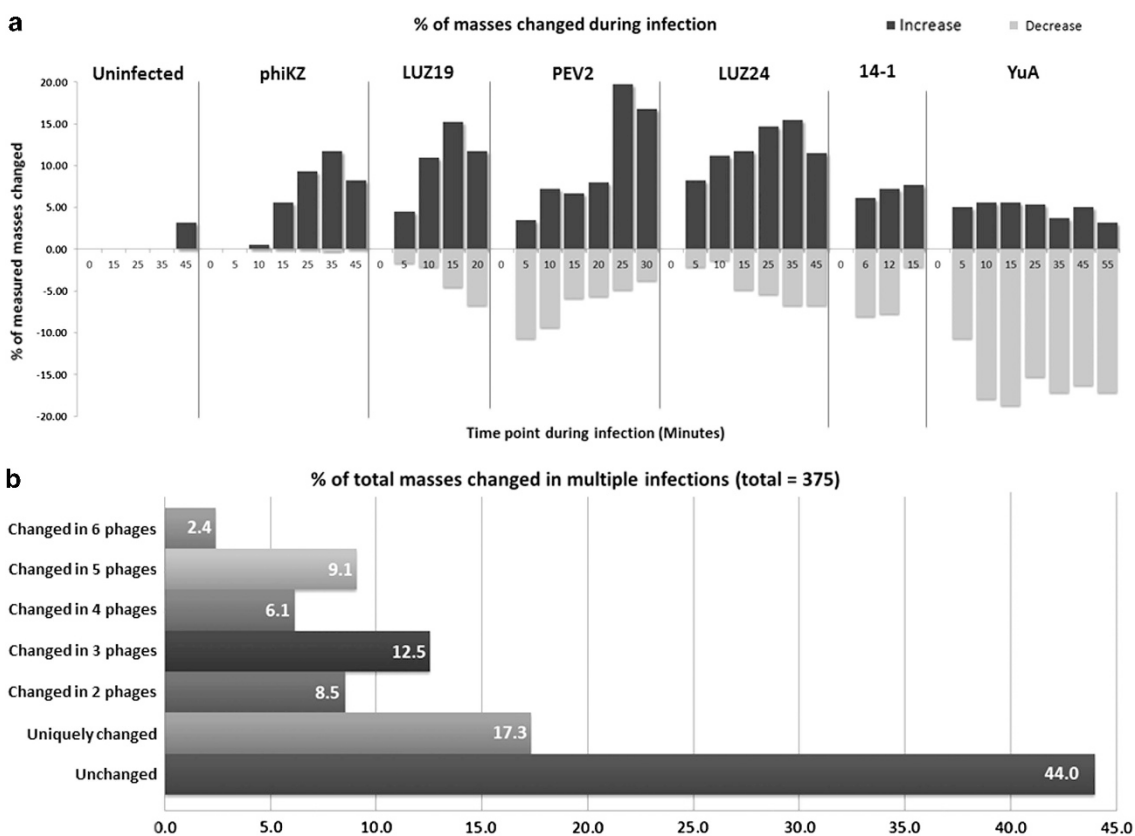


Figure 2 (a) Percentage of altered *Pseudomonas* metabolites during the course of infection of *P. aeruginosa* with six different phage clades (P -value ≤ 0.05 and $\log_2(\text{fold change}) \leq -0.5$ or ≥ 0.5). Fold changes were determined by comparison of metabolite levels before infection against the mentioned time point during infection. (b) Percentage of metabolites changed in multiple phage infections, metabolites were considered significantly changed when P -value ≤ 0.05 and $\log_2(\text{fold change}) \leq -0.5$ or ≥ 0.5 .

analyses over the different time points were combined (Figure 4).

Most of the enriched pathways can be linked to specific requirements during phage replication. First, most negatively impacted pathways are related to amino-acid metabolism, with a decrease in the metabolism of 14/20, 11/20, 10/20, 4/20 and 3/20 amino acids (and precursors) during the infection of YuA, 14-1, PEV2, LUZ19 and LUZ24, respectively (Figure 4). This decrease can be explained by either a decreased production or an increased incorporation

of these amino acids in proteins, not compensated by increased production. An increased consumption of amino acids during phage particle formation seems the most logical hypothesis. However, not all phages deplete amino acids to an equal extent, whereas the giant phage phiKZ does not even exhibit this decrease. This observation indicates different levels of dependency on the host cell resources, as discussed later.

Second, multiple pathways involved in nucleotide metabolism have been influenced. The pyrimidine

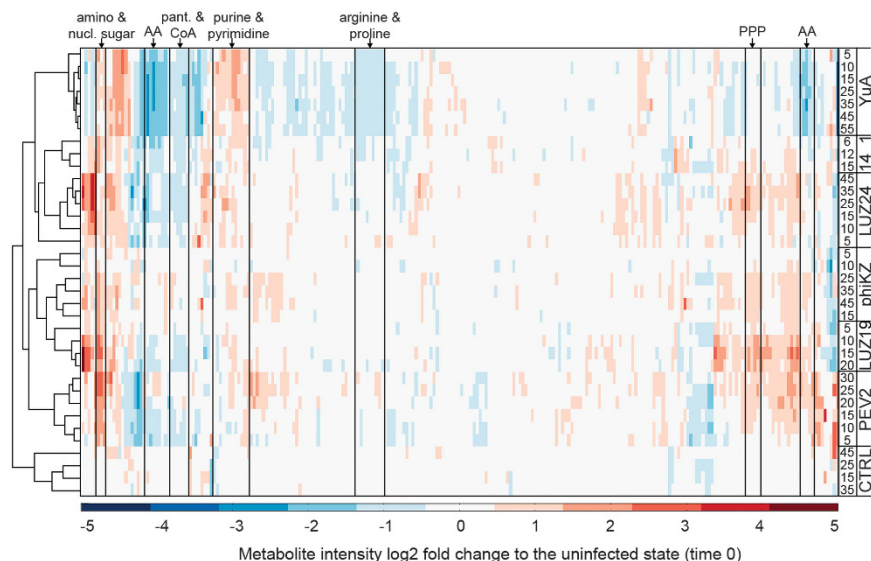


Figure 3 Hierarchical clustering based on correlations between mean metabolite fold change vectors reveals phage-specific changes in host metabolism. Color bar indicates the fold change of different metabolites (columns) for the different samples (rows). On the left is the hierarchical tree showing the relation between the different samples. On the right is the different time points and infecting phage are indicated for each row of metabolite fold changes. On the top is the corresponding pathways are shown for clusters of metabolites. AA, amino acids; nucl, nucleotide; pant, Panthotenate; PPP, pentose phosphate pathway.

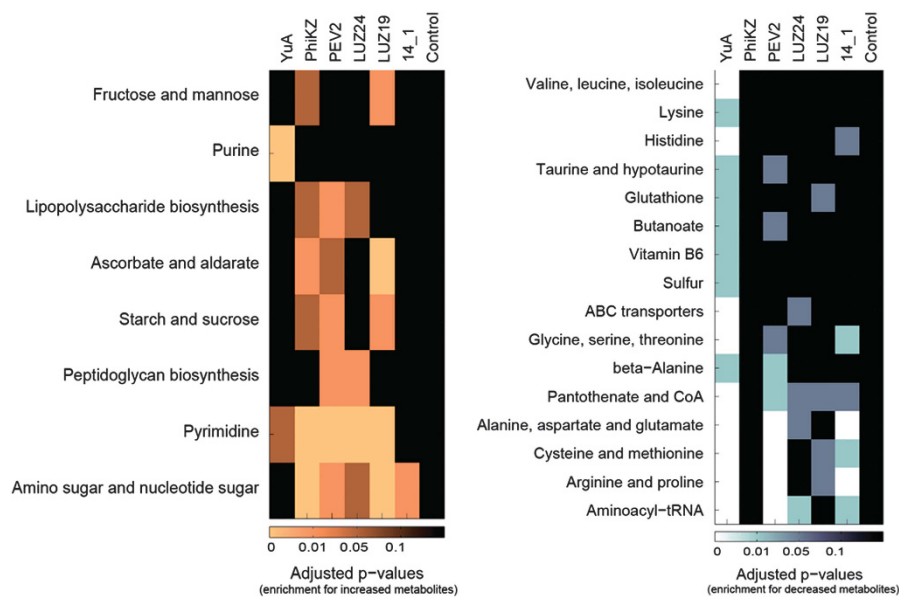


Figure 4 Metabolic pathway enrichment for different phages. The results for the enrichment analysis are shown for all six phages (columns) and for all respectively significantly decreased and increased pathways (rows). The color scale indicates the cutoff for the *P*-values. Note, pathways are only shown if at least one time point shows an enrichment *P*-value < 0.05.

pathway, which produces the required pyrimidine nucleotides for DNA replication, is enriched for increased metabolites for all analyzed phages, except for 14-1 (Figure 4). Using a Venn diagram, the overlap in changed metabolites between phages was visualized (Supplementary Figure S3). Most of the final pyrimidine nucleotides are increased in all infections, whereas the intermediates only increase for phiKZ and even decrease for PEV2, LUZ24 and YuA (Supplementary Figure S3). Interestingly, the purine metabolism was only enriched for increased metabolites during infection by YuA. This hints at a difference in the need/consumption of pyrimidine versus purine nucleotides during phage infection. Metabolite levels of glutathione metabolism are decreased by both LUZ19 and YuA (Supplementary Figure S2). Glutathione is essential for oxidative stress protection and increased activity of ribonucleotide reductases in nucleotide metabolism (Masip *et al.*, 2006). These enzymes catalyze the formation of deoxyribonucleotides from ribonucleotides, an essential step for phage DNA replication.

Metabolites of pantothenate and coenzyme A (CoA) metabolism are decreased in all phages, except phiKZ (Figure 4). CoA has an important role in many host pathways that supply essential components and energy to the cell (Leonardi *et al.*, 2005). The enrichment of the pantothenate and CoA pathway among decreased metabolites would slow down the host metabolism. This may be explained by the phage-induced host metabolism take-over or shut-down. However, although the metabolite levels of pantoate and aspartate levels are indeed decreased, some intermediate metabolites and CoA levels are even increased by certain phages, for example, PEV2, LUZ24 and YuA (Supplementary Figure S4). In these cases, the observed decrease in CoA metabolism could also be caused by increased CoA consumption.

The third pathway affected for all phages, except YuA, is the amino sugar and nucleotide sugar metabolism (Supplementary Figure S5). Nucleotide sugars are the building blocks for peptidoglycan and lipopolysaccharides, required for cell growth and division. Multiple examples exist of phage proteins that inhibit cell division or cell wall biosynthesis, such as lysis protein E of phiX174 (Bernhardt *et al.*, 2001) or the kil proteins in phages Mu (Waggoner *et al.*, 1989), P22 (Semerjian *et al.*, 1989), lambda (Sergueev *et al.*, 2001) and Sf6 (Casjens *et al.*, 2004). Homologs of these proteins share only low levels of sequence similarity (Sau *et al.*, 2008), and have not yet been identified in these *Pseudomonas* phages. However, the increased levels in the nucleotide sugars appears to be indicative of the presence of phage proteins inhibiting cell division or cell wall biosynthesis. This is further illustrated by the enrichment of peptidoglycan and lipopolysaccharide biosynthesis during PEV2, LUZ24 and phiKZ infection. In fact, *Phikzlikevirus* members encode a tubulin-like protein (Kraemer *et al.*, 2012), which positions the phage DNA in the center of the cell and

induces an arrest in host cell division during infection (Ceyssens *et al.*, 2014). Other cell division inhibiting early proteins were also identified in LUZ7, an *N4likevirus* like PEV2 (Wagemans *et al.*, 2014).

Most of the remaining pathways enriched for increased metabolites are involved in host carbohydrate metabolism, which produces the required building blocks for biomass production, however, the affected carbon sources vary between phages (Figure 4). Interestingly, none of the central carbon metabolism pathways (for example, TCA cycle, glycolysis) were enriched. To conclude, this pathway enrichment analysis reveals a primarily phage-specific impact on host physiology, a central need for pyrimidine nucleotides and a widespread accumulation of nucleotide sugars during phage infection.

Host stress metabolites reveal phage-specific impact on different stress responses

In response to different stresses, *P. aeruginosa* produces secondary messenger molecules, which enable cell-to-cell communication and coordinated responses (Jimenez *et al.*, 2012). To assess if phage infection would trigger these host stress responses, the detected metabolites were analyzed. Although many of them were not detected (for example, AHLs, c-di-GMP and cAMP), both ppGpp and *Pseudomonas* quinolone signal (PQS) could be analyzed.

First, ppGpp controls the bacterial growth rate by inhibiting the production of ribosomal RNA (Potrykus and Cashel, 2008; Potrykus *et al.*, 2011). It also fine tunes the metabolism by transcriptional regulation of enzymes involved in amino-acid metabolism and binding of enzymes involved in nucleotide metabolism (Gallant *et al.*, 1971; Hochstadt-Ozer and Cashel, 1972; Potrykus and Cashel, 2008). High levels of this molecule are linked to the stringent response, which occurs on exposure to amino-acid starvation or heat shock (Traxler *et al.*, 2008; Hauryliuk *et al.*, 2015). The level of this molecule increases during LUZ19, 14-1 and YuA infection, whereas it remains stable for phiKZ and even decreases for LUZ24 and PEV2 (<http://www.biw.kuleuven.be/LoGTdb/phageBiosystems/Pathways.aspx?cpd=C01228>). This clear distinction between the phages does not appear to be correlated to other observed metabolic differences, such as the decreased amino-acid levels in multiple phages (YuA, 14-1, PEV2, LUZ19 and LUZ24). This seems to indicate an active interference in the stringent response during phage infection.

The second stress metabolite, the 'PQS', triggers autolysis and DNA fragmentation, whereas simultaneously lowering the metabolic activity in undamaged bacteria and increasing the protection against oxidative stress (D'Argenio *et al.*, 2002). It has a central selective role for the survival of the fittest (Häussler and Becker, 2008). The PQS metabolite

level increases during YuA, 14-1 and LUZ24 infection (<http://www.biw.kuleuven.be/LoGTdb/phageBiosystems/Pathways.aspx?cpd=C11848>), which hints at a host response aimed to protect the fittest (uninfected) cells by slowing down metabolism and killing the susceptible (infected) cells. Surprisingly, PQS levels are not increased upon phiKZ, LUZ19 and PEV2 infection. Either the activation of the PQS system is not a general host response or these phages have evolved unknown mechanisms to block PQS synthesis.

Observed correlations between the phage-specific metabolic responses and predicted AMGs

To investigate what is causing the phage-specific impact on host physiology, all phage genomes were screened for potential AMGs using the bioinformatics tool BLASTn (Table 2) (Altschul et al., 1990). The number of potential AMGs identified was limited in all phages (around 3% of all genes) and most were Class I AMGs predicted to be involved in nucleotide metabolism. Their presence likely explains the common impact on pyrimidine metabolism in most phages, corresponding to the central need for nucleotides in viral genome replication. In fact, the increased levels of metabolites in this pathway, as well as the amino sugar and nucleotide sugar metabolism, were also hypothesized from a

metagenomic screen for enriched viral auxiliary genes from the Global Ocean Survey (Enav et al., 2014). The authors hypothesized that viruses carry these metabolic genes to expand the nucleotide pool in two ways, by recycling the nucleotides of the cellular genome and transcriptome (Powell et al., 1992; Ueno and Yonesaki, 2004; Lavigne et al., 2013) and/or by directing the host metabolism to provide substrates for *de novo* synthesis (Thompson et al., 2011).

Indeed, the giant myovirus phiKZ redirects the host metabolism to provide substrates for *de novo* synthesis (Figure 5). The genome of this giant virus contains seven AMGs, which can be linked to the pyrimidine pathway (Table 2). Directly after infection, the intermediates of *de novo* pyrimidine synthesis show a clear increase (for example, *N*-carbamoyl-L-aspartate, (S)-dihydroorotate), followed by a slow increase in the nucleotide monophosphates (Figure 5). Considering the coding potential of this giant virus (280.3 kb) and its host-independent transcriptional regulation scheme (Ceyssens et al., 2014), it is tempting to rationalize a similar independence of available host resources at the metabolome level. Indeed, phiKZ appears to have no influence on the cell's metabolites during early infection, but approximately 10% of all annotated metabolites gradually accumulate during late infection (Figure 2a).

Table 2 Predicted AMGs present in phage genomes as well as their class

Phage	Host DNA degradation?	tRNA in phage genome	Predicted AMGs in phage genome (using blastN)				
			ORF	Predicted function	E-value	Pathway	Class
LUZ19	Yes	—	gp23	Endonuclease_7	5×10^{-10}	Nucleotide	Class II
LUZ24	Probable	2	gp19	L-glutamine-D-fructose-6-phosphate amidotransferase	2×10^{-6}	Amino acid/ carbohydrate	Class I
		Pro Asn	gp21	Glutathione synthase	2×10^{-3}	Glutathione	Class I
			gp22	Gamma-glutamyl cyclotransferase	2×10^{-4}	Glutathione	Class I
			gp35	Endonuclease_7	5×10^{-15}	Nucleotide	Class II
PEV2	ND	—	gp39	Deoxycytidylate deaminase	1×10^{-19}	Nucleotide	Class I
			gp81	Deoxyuridinetriphosphatase	1×10^{-21}	Nucleotide	Class I
14-1	ND	—	gp57	PnkP, polynucleotide kinase	3×10^{-5}	Amino acid	Class II
			gp59	FAD-dependent thymidylate synthase	8×10^{-21}	Nucleotide	Class I
phiKZ	ND	6	gp4	Dihydrofolate reductase	5×10^{-22}	Folate	Class I
		Pro Asn Asp Leu Thr Met	gp188	Thymidilate kinase	6×10^{-12}	Nucleotide	Class I
			gp214	Deoxycytidine triphosphate deaminase	4×10^{-51}	Nucleotide	Class I
			gp235	Thymidilate synthase	4×10^{-26}	Nucleotide	Class I
			gp260	dCMP deaminase	3×10^{-14}	Nucleotide	Class I
			gp305	Ribonucleotide reductase β chain	2×10^{-16}	Nucleotide/ glutathione	Class I
			gp306	Ribonucleotide reductase α chain	2×10^{-99}	Nucleotide/ glutathione	Class I
YuA	ND	—	gp6	RecD exonuclease V, alpha subunit	1×10^{-98}	Nucleotide	Class II
			gp7	Ribonucleotide reductase	9×10^{-150}	Nucleotide/ glutathione	Class I
			gp11	Threonine dehydratase	5×10^{-6}	Amino acid	Class I
			gp17	Thymidilate synthase and pyrimidine hydroxymethylase	2×10^{-83}	Nucleotide	Class I
			gp23	dCMP deaminase	8×10^{-21}	Nucleotide	Class I

Abbreviations: AMG, auxiliary metabolic gene; ND, not determined; ORF, open reading frame; tRNA, transfer RNA.

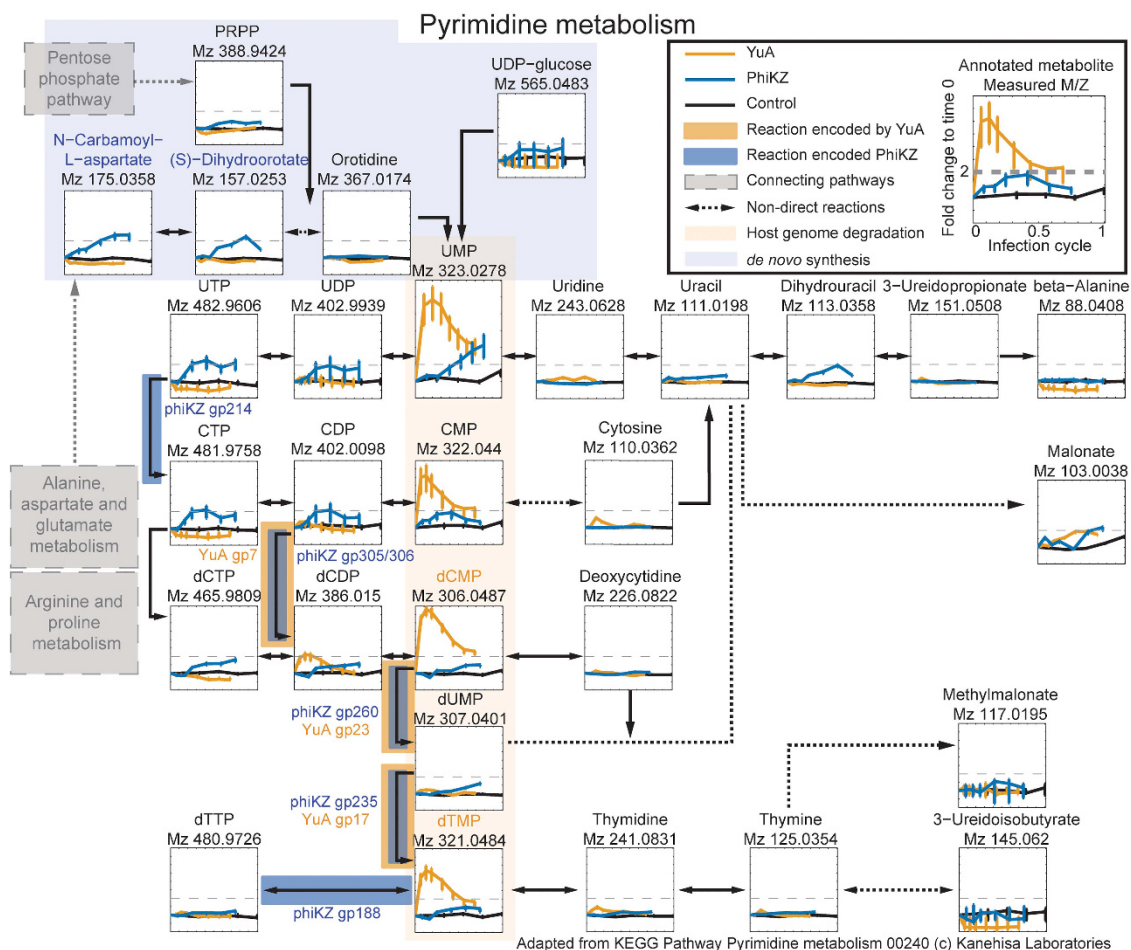


Figure 5 Both the strategy of recycling and *de novo* synthesis of pyrimidine nucleotides are present in the set of phages. Graphs show the fold changes of metabolites in the pyrimidine pathway at different stages of infection (black-control, orange-YuA and blue-phiKZ). YuA recycles nucleotides (orange shade), characterized by a rapid increase of nucleotides. PhiKZ showed an increased *de novo* synthesis (blue shade), characterized by an increase in early building blocks. The y axis shows the fold change, x axis shows the time points during infection (in minutes), annotated metabolite name and ion mass are shown above the graph. The colored squares indicate the enzymatic reactions encoded by YuA (orange) and phiKZ (blue). The metabolites mentioned in the text are also highlighted.

As the other phages contain smaller genomes, they may lack the coding capacity to generate a functioning host metabolism and rely more on depletion of the host resources. This may explain the immediate increase in nucleotide monophosphates (for example, dTMP and dCMP) in the pyrimidine metabolism during the infection of siphovirus YuA. Most likely, this is the result of host genome degradation, because of unchanged levels of the above mentioned intermediates (Figure 5) and the presence of a predicted exonuclease (gp6) in the YuA genome (Table 2). In comparison with phiKZ, the smaller phage YuA (58.6 kb) uses a ‘leeching’ strategy, aimed at harvesting metabolites from the host. In fact, after infection an immediate negative effect on approximately 17% of all measured metabolites is observed, which results in a distinct metabolic effect for this phage (Figure 3) and a high number of negatively impacted pathways (Figure 4). However, the immediate degradation of the host genome may also explain the overall negative effect observed in YuA. This is a

clear example of how the presence of a single AMG, in this case a nuclease, results in a distinct different metabolic impact.

A second example of the role AMGs might have, has been found when comparing the impact of LUZ19 and LUZ24. At first sight, these two phages show very similar percentages of metabolite increase and decrease during infection (Figure 2a), which may be explained by their relative close relationship within the population network (Figure 1). Both phages cause an increase in nucleotide levels after the first third of infection (Supplementary Figure S6). As they both encode an endonuclease, gp23 for LUZ19 and gp35 for LUZ24 (Table 2), the observed increase is likely caused by host genome degradation, which has already been experimentally shown for LUZ19 (but not LUZ24) at the start of viral genome replication (after the first third of infection) (Lavigne *et al.*, 2013). However, the hierarchical clustering revealed more differences at the metabolite level between LUZ24 and LUZ19 (Figure 3).

A comparison of the encoded AMG content revealed three AMGs that are present in LUZ24, but absent in LUZ19 (Table 2).

LUZ24 gp19 is a predicted L-glutamine-D-fructose-6-phosphate amidotransferase (also called glucosamine-6-phosphate synthase, *glmS*). This protein catalyzes the rate-limiting enzymatic step in *de novo* biosynthesis of UDP-GlcNAc, the activated form of N-acetylglucosamine (Milewski, 2002). This metabolite is required for the biosynthesis of peptidoglycan and lipopolysaccharide (Mirelman and Nuchamowitz, 1979; King *et al.*, 2009). Late in LUZ24 infection, the level of UDP-GlcNAc (C00043) is indeed significantly increased ($FC_{35 \text{ minutes}} = 1$), which is not observed for LUZ19. This indicates that LUZ24 gp19 is indeed a novel functional glucosamine-6-phosphate synthase. The presence of this AMG resulted in a lower enrichment of the amino sugar metabolism for increased metabolites in LUZ24, compared with LUZ19 (Supplementary Figure S2). Most likely, this is the result of a decreased accumulation of the precursors before this rate limiting enzymatic step. Although no stable lysogenic isolates could be obtained for this phage (Ceyssens *et al.*, 2008), it is genetically homologous (71% sequence identity) to the temperate phage PaP3 (Tan *et al.*, 2007). This AMG could be an artifact of its former temperate nature, where it would yield a fitness benefit to the host during lysogeny (Feiner *et al.*, 2015). The two other AMGs, solely present in LUZ24, are involved in glutathione metabolism (Table 2). Metabolites of this pathway are only decreased during LUZ19 infection, whereas they remain stable during LUZ24 infection. This decrease is likely caused by oxidative stress because of phage progeny production, the AMGs in LUZ24 can compensate this drop and thus reduce oxidative stress (Figure 4).

Phage 14-1 encodes two predicted AMGs, one involved in pyrimidine metabolism and a homolog to the T4 polynucleotide kinase (PnkP) (Table 2). During infection, 14-1 exhibits both increased (7.2%) and decreased (7.7%) metabolites (Figure 2a). Despite the presence of this AMG, it is the only phage where the pyrimidine pathway is not enriched for increased metabolites (Figure 4). In T4, PnkP repairs host-induced cleavage of host tRNAs (for example, lysine) by ribotoxins to circumvent the host's attempt to block T4 protein synthesis (Amitsur *et al.*, 1987; Wang *et al.*, 2015). Metabolites associated with the amino-acid metabolism are decreased early in the short 14-1 infection (<15 min), whereas towards the end of infection this negative effect is less pronounced (Supplementary Figure S2). These observations indicate the presence of the PnkP homolog may enable 14-1 to respond to a triggered host defense and complete its rapid infection cycle.

The last phage, PEV2 belongs to the same genus (*N4likevirus*) as roseophage Φ 2047B, studied by Ankrah *et al.* (2014). As both phages share a general genome organization, similarity in the host response

was expected. Indeed, after one infection cycle, an increase is observed for approximately 20% of the detected metabolites, whereas only a small fraction (4.8%) was significantly decreased (Figure 2a). However, early in infection, up to 10% of measured metabolites were decreased, something which was not observed for the roseophage (Figure 2a). This is due to a drop in amino-acid-related metabolites early in infection, which is restored over time. PEV2 encodes only two predicted AMGs, which fail to explain the observed effects on amino-acid metabolism (Supplementary Figure S2).

Although the identified and described AMGs already offer some explanations for the phage-specific metabolic effects, many other effects cannot be attributed to predicted AMGs at this time. Given the high number of encoded viral genes that lack any functional prediction in all of these phages, we can speculate on the significant importance of unknown, 'non-enzymatic' peptides in metabolism take-over. Such AMGs could technically be defined as Class II AMGs, although they lack any direct metabolic function. More and more of such peptides are being identified, for example, the interaction of an early protein of LUZ7 (gp30) with a protein involved in polyamine metabolism (PA4114) (Wagemans *et al.*, 2014) or the early protein of phiKMV (gp9), which is hypothesized to impact the TCA cycle (Roucourt *et al.*, 2009). These findings emphasize the need for more efforts to characterize the function of such small, unknown viral gene products.

An open access database enables straightforward interpretation and interactive analysis of the metabolomics data

Unfortunately, metabolomics data sets of phage–host systems are scarce and hardly accessible, despite the fact that the entire community could benefit from such large data sets. For this reason, an interactive database was set up providing open access to the data and a straightforward to use, visual interface to analyze and compare them (<http://www.biw.kuleuven.be/LoGTdb/phageBiosystems/Home.aspx>). The data interpretation is possible at different levels: comparative analysis between phages, phage-specific interpretation and pathway/metabolite-tailored visualization. These tools should enable researchers to look at specific metabolites/responses upon phage infection. Finally, this database is a first step toward an online platform capable of integrating proteomics, metabolomics and transcriptomics data sets, which, because of the technological advances in these fields, enables the study of phage infection at a systems level.

Conclusions

Implications for phage biology

In this work, we provide a detailed insight into the changing metabolic content of phage-infected

P. aeruginosa cells, within a single infection cycle, and conclude that the phage-specific alterations of the host metabolism are more than a mere depletion of the host metabolites. A clear distinction can be made between 'leeching' phages, which take all existing resources for viral replication (for example, YuA), and phages that actively modulate the metabolism, by redirecting the cell's metabolism to produce new resources, required for phage production (for example, phiKZ). The great diversity in genetic features of each individual phage is the driver for this metabolic diversity. We further show that specific metabolic pathways, targeted by the AMGs, are statistically enriched in the set of metabolites changing upon infection. Therefore, each specific set of AMGs will result in a unique metabolic phenotype after infection. From a more philosophical perspective, this altered metabolic state of the phage-infected cell is consistent with the definition of viral life (virocell concept) (Forterre, 2013).

Implications for global ecosystem and fluxes studies

The presence of viruses in microbial communities impacts nutrient fluxes. Recently, a model was presented which demonstrated the impact of virus infection on marine food webs and stressed the need to take the viral presence into account (Weitz *et al.*, 2015). However, as the (current consensus is that the) virome contains an almost unlimited source of AMGs from which phages retain those beneficial for their needs (Sharon *et al.*, 2011), not only the occurrence of phage infection but also the diversity of the phages present will impact the net metabolic effect of phage infections in complex bacterial populations. This is an additional element that should be considered when trying to understand such complex systems and the role phages have in them, such as in global nutrient fluxes.

Implications for biotechnology

Finally, this study provides a valuable resource to investigate the link between the metabolic effects of a phage and its encoded AMGs and the search for unknown 'non-enzymatic' AMGs. To catalyze the research, an interactive database (<http://www.biw.kuleuven.be/LoGTdb/phageBiosystems/Home.aspx>) was set up to allow fast visualization of the data depending on the research question. In future, this database could be expanded with data from single phage gene expression, transcriptome and protein interaction data to allow a thorough analysis of phage infection at the systems' biology level. With the newly developed phenomics technique (Sanchez *et al.*, 2015), we expect the discovery of phage-encoded AMGs to boom in the coming years. Such 'metabolic modulators' could provide key tools toward novel biotechnological applications in the advanced metabolic tailoring of bacteria.

Conflict of Interest

The authors declare no conflict of interest.

Acknowledgements

J De Smet holds a predoctoral fellowship of the 'Agentschap voor Innovatie door Wetenschap en Technologie in Vlaanderen' (IWT, Belgium). This research was also supported by grant G.0323.09 from the FWO and the KULeuven project GOA 'Phage Biosystems'.

References

- Altschul SF, Gish W, Miller W, Myers EW, Lipman DJ. (1990). Basic local alignment search tool. *J Mol Biol* **215**: 403–410.
- Amitsur M, Levitz R, Kaufmann G. (1987). Bacteriophage T4 anticodon nuclease, polynucleotide kinase and RNA ligase reprocess the host lysine tRNA. *EMBO J* **6**: 2499–2503.
- Ankrah NYD, May AL, Middleton JL, Jones DR, Hadden MK, Gooding JR *et al.* (2014). Phage infection of an environmentally relevant marine bacterium alters host metabolism and lysate composition. *ISME J* **8**: 1089–1100.
- Bergh O, Børsheim KY, Bratbak G, Heldal M. (1989). High abundance of viruses found in aquatic environments. *Nature* **340**: 467–468.
- Bernhardt TG, Struck DK, Young R. (2001). The lysis protein E of phi X174 is a specific inhibitor of the MraY-catalyzed step in peptidoglycan synthesis. *J Biol Chem* **276**: 6093–6097.
- Bosco MB, Machtey M, Iglesias AA, Aleanzi M. (2009). UDPglucose pyrophosphorylase from *Xanthomonas* spp. Characterization of the enzyme kinetics, structure and inactivation related to oligomeric dissociation. *Biochimie* **91**: 204–213.
- Van den Bossche A, Ceyssens P-J, De Smet J, Hendrix H, Bellon H, Leimer N *et al.* (2014). Systematic identification of hypothetical bacteriophage proteins targeting key protein complexes of *Pseudomonas aeruginosa*. *J Proteome Res* **13**: 4446–4456.
- Breitbart M, Thompson LR, Suttle CA, Sullivan MB. (2007). Exploring the vast diversity of marine viruses. *Oceanography* **2**: 135–139.
- Casjens S, Winn-Stapley DA, Gilcrease EB, Morona R, Kühlewein C, Chua JEH *et al.* (2004). The chromosome of *Shigella flexneri* bacteriophage Sf6: complete nucleotide sequence, genetic mosaicism, and DNA packaging. *J Mol Biol* **339**: 379–394.
- Ceyssens P-J, Hertveldt K, Ackermann HW, Noben JP, Demeke M, Volckaert G *et al.* (2008). The intron-containing genome of the lytic *Pseudomonas* phage LUZ24 resembles the temperate phage PaP3. *Virology* **377**: 233–238.
- Ceyssens P-J, Lavigne R. (2010). Bacteriophages of *Pseudomonas*. *Future Microbiol* **5**: 1041–1055.
- Ceyssens P-J, Mesyanzhinov V, Sykilinda N, Briers Y, Roucourt B, Lavigne R *et al.* (2008). The genome and structural proteome of YuA, a new *Pseudomonas aeruginosa* phage resembling M6. *J Bacteriol* **190**: 1429–1435.

- Ceyssens P-J, Minakhin L, Van den Bossche A, Yakunina M, Klimuk E, Blasdel B *et al.* (2014). Development of giant bacteriophage ϕ KZ is independent of the host transcription apparatus. *J Virol* **88**: 10501–10510.
- Ceyssens P-J, Miroshnikov K, Mattheus W, Krylov V, Robben J, Noben J-P *et al.* (2009). Comparative analysis of the widespread and conserved PB1-like viruses infecting *Pseudomonas aeruginosa*. *Environ Microbiol* **11**: 2874–2883.
- D'Argenio DA, Calfee MW, Rainey PB, Pesci EC. (2002). Autolysis and autoaggregation in *Pseudomonas aeruginosa* colony morphology mutants. *J Bacteriol* **184**: 6481–6489.
- Danovaro R, Dell'Anno A, Corinaldesi C, Magagnini M, Noble R, Tamburini C *et al.* (2008). Major viral impact on the functioning of benthic deep-sea ecosystems. *Nature* **454**: 1084–1087.
- Ebrecht AC, Ascención Díez MD, Piattoni CV, Guerrero SA, Iglesias AA. (2015). The UDP-glucose pyrophosphorylase from *Giardia lamblia* is redox regulated and exhibits promiscuity to use galactose-1-phosphate. *Biochim Biophys Acta* **1850**: 88–96.
- Ehebauer MT, Zimmermann M, Jakobi AJ, Noens EE, Laubitz D, Cichocki B *et al.* (2015). Characterization of the mycobacterial Acyl-CoA carboxylase Holo complexes reveals their functional expansion into amino acid catabolism, Schnappinger D (ed). *PLOS Pathog* **11**: e1004623.
- Enav H, Mandel-Gutfreund Y, Béjà O. (2014). Comparative metagenomic analyses reveal viral-induced shifts of host metabolism towards nucleotide biosynthesis. *Microbiome* **2**: 9.
- Falkowski PG, Fenchel T, Delong EF. (2008). The microbial engines that drive Earth's biogeochemical cycles. *Science* **320**: 1034–1039.
- Feiner R, Argov T, Rabinovich L, Sigal N, Borovok I, Herskovits AA. (2015). A new perspective on lysogeny: prophages as active regulatory switches of bacteria. *Nat Rev Microbiol* **13**: 641–650.
- Fendt S-M, Buescher JM, Rudroff F, Picotti P, Zamboni N, Sauer U. (2010). Tradeoff between enzyme and metabolite efficiency maintains metabolic homeostasis upon perturbations in enzyme capacity. *Mol Syst Biol* **6**: 356.
- Forterre P. (2013). The virocell concept and environmental microbiology. *ISME J* **7**: 233–236.
- Frank JA, Lorimer D, Youle M, Witte P, Craig T, Abendroth J *et al.* (2013). Structure and function of a cyanophage-encoded peptide deformylase. *ISME J* **7**: 1150–1160.
- Fuhrer T, Heer D, Begemann B, Zamboni N. (2011). High-throughput, accurate mass metabolome profiling of cellular extracts by flow injection-time-of-flight mass spectrometry. *Anal Chem* **83**: 7074–7080.
- Gallant J, Irr J, Cashel M. (1971). The mechanism of amino acid control of guanylate and adenylate biosynthesis. *J Biol Chem* **246**: 5812–5816.
- Hargreaves KR, Kropinski AM, Clokie MR. (2014). Bacteriophage behavioral ecology: how phages alter their bacterial host's habits. *Bacteriophage* **4**: e29866.
- Hatfull GF. (2008). Bacteriophage genomics. *Curr Opin Microbiol* **11**: 447–453.
- Hauryliuk V, Atkinson GC, Murakami KS, Tenson T, Gerdes K. (2015). Recent functional insights into the role of (p)ppGpp in bacterial physiology. *Nat Rev Microbiol* **13**: 298–309.
- Häussler S, Becker T. (2008). The pseudomonas quinolone signal (PQS) balances life and death in *Pseudomonas aeruginosa* populations. *PLoS Pathog* **4**: e1000166.
- Hochstadt-Ozer J, Cashel M. (1972). The regulation of purine utilization in bacteria. V. Inhibition of purine phosphoribosyltransferase activities and purine uptake in isolated membrane vesicles by guanosine tetraphosphate. *J Biol Chem* **247**: 7067–7072.
- Holloway BW. (1955). Genetic recombination in *Pseudomonas aeruginosa*. *J Gen Microbiol* **13**: 572–581.
- Hurwitz BL, Brum JR, Sullivan MB. (2015). Depth-stratified functional and taxonomic niche specialization in the 'core' and 'flexible' Pacific Ocean Virome. *ISME J* **9**: 472–484.
- Hurwitz BL, Hallam SJ, Sullivan MB. (2013). Metabolic reprogramming by viruses in the sunlit and dark ocean. *Genome Biol* **14**: R123.
- Jimenez PN, Koch G, Thompson JA, Xavier KB, Cool RH, Quax WJ. (2012). The multiple signaling systems regulating virulence in *Pseudomonas aeruginosa*. *Microbiol Mol Biol Rev* **76**: 46–65.
- King JD, Kocíncová D, Westman EL, Lam JS. (2009). Review: lipopolysaccharide biosynthesis in *Pseudomonas aeruginosa*. *Innate Immun* **15**: 261–312.
- Kraemer JA, Erb ML, Waddling CA, Montabana EA, Zehr EA, Wang H *et al.* (2012). A phage tubulin assembles dynamic filaments by an atypical mechanism to center viral DNA within the host cell. *Cell* **149**: 1488–1499.
- Lammens E, Ceyssens PJ, Voet M, Hertveldt K, Lavigne R, Volckaert G. (2009). Representational Difference Analysis (RDA) of bacteriophage genomes. *J Microbiol Methods* **77**: 207–213.
- Lavigne R, Lecoutere E, Wagemans J, Cenens W, Aertsen A, Schoofs L *et al.* (2013). A multifaceted study of *Pseudomonas aeruginosa* shutdown by virulent podovirus LUZ19. *MBio* **4**: e00061–13.
- Leonardi R, Zhang Y-M, Rock CO, Jackowski S. (2005). Coenzyme A: back in action. *Prog Lipid Res* **44**: 125–153.
- Leplae R, Hebrant A, Wodak SJ, Toussaint A. (2004). ACLAME: a CLAssification of Mobile genetic Elements. *Nucleic Acids Res* **32**: D45–D49.
- Lindell D, Jaffe JD, Johnson ZI, Church GM, Chisholm SW. (2005). Photosynthesis genes in marine viruses yield proteins during host infection. *Nature* **438**: 86–89.
- Link H, Kochanowski K, Sauer U. (2013). Systematic identification of allosteric protein-metabolite interactions that control enzyme activity *in vivo*. *Nat Biotechnol* **31**: 357–361.
- Martiny AC, Huang Y, Li W. (2009). Occurrence of phosphate acquisition genes in *Prochlorococcus* cells from different ocean regions. *Environ Microbiol* **11**: 1340–1347.
- Masip L, Veeravalli K, Georgiou G. (2006). The many faces of glutathione in bacteria. *Antioxid Redox Signal* **8**: 753–762.
- Mesyanzhinov VV, Robben J, Grymonprez B, Kostyuchenko VA, Bourkaltseva MV, Sykilinda NN *et al.* (2002). The genome of bacteriophage ϕ KZ of *Pseudomonas aeruginosa*. *J Mol Biol* **317**: 1–19.
- Milewski S. (2002). Glucosamine-6-phosphate synthase—the multi-facets enzyme. *Biochim Biophys Acta* **1597**: 173–192.
- Miller ES, Kutter E, Mosig G, Arisaka F, Kunisawa T, Rieger W. (2003). Bacteriophage T4 genome. *Microbiol Mol Biol Rev* **67**: 86–156. (table of contents).

- Mirelman D, Nuchamowitz Y. (1979). Biosynthesis of peptidoglycan in *Pseudomonas aeruginosa*. 1. The incorporation of peptidoglycan into the cell wall. *Eur J Biochem* **94**: 541–548.
- Oberhardt MA, Puchalka J, Fryer KE, Martins dos Santos VAP, Papin JA. (2008). Genome-scale metabolic network analysis of the opportunistic pathogen *Pseudomonas aeruginosa* PAO1. *J Bacteriol* **190**: 2790–2803.
- Oliveira AP, Ludwig C, Picotti P, Kogadeeva M, Aebersold R, Sauer U. (2012). Regulation of yeast central metabolism by enzyme phosphorylation. *Mol Syst Biol* **8**: 623.
- Paul JH, Sullivan MB. (2005). Marine phage genomics: what have we learned? *Curr Opin Biotechnol* **16**: 299–307.
- Potrykus K, Cashel M. (2008). (p)ppGpp: still magical? *Annu Rev Microbiol* **62**: 35–51.
- Potrykus K, Murphy H, Philippe N, Cashel M. (2011). ppGpp is the major source of growth rate control in *E. coli*. *Environ Microbiol* **13**: 563–575.
- Powell IB, Tulloch DL, Hillier AJ, Davidson BE. (1992). Phage DNA synthesis and host DNA degradation in the life cycle of *Lactococcus lactis* bacteriophage c6A. *J Gen Microbiol* **138**: 945–950.
- Qimron U, Marintcheva B, Tabor S, Richardson CC. (2006). Genomewide screens for *Escherichia coli* genes affecting growth of T7 bacteriophage. *Proc Natl Acad Sci USA* **103**: 19039–19044.
- Rabinowitz JD. (2007). Cellular metabolomics of *Escherichia coli*. *Expert Rev Proteomics* **4**: 187–198.
- Rohwer F, Youle M. (2011). Consider something viral in your research. *Nat Rev Microbiol* **9**: 308–309.
- Roucourt B, Lavigne R. (2009). The role of interactions between phage and bacterial proteins within the infected cell: a diverse and puzzling interactome. *Environ Microbiol* **11**: 2789–2805.
- Roucourt B, Lecoutere E, Chibeu A, Hertveldt K, Volckaert G, Lavigne R. (2009). A procedure for systematic identification of bacteriophage-host interactions of *P. aeruginosa* phages. *Virology* **387**: 50–58.
- Sanchez SE, Cuevas DA, Rostron JE, Liang TY, Pivaroff CG, Haynes MR *et al*. (2015). Phage phenomics: physiological approaches to characterize novel viral proteins. *J Vis Exp* **11**: e52854.
- Sau S, Chatteraj P, Ganguly T, Chanda PK, Mandal NC. (2008). Inactivation of indispensable bacterial proteins by early proteins of bacteriophages: implication in antibacterial drug discovery. *Curr Protein Pept Sci* **9**: 284–290.
- Schulz JC, Zampieri M, Wanka S, von Mering C, Sauer U. (2014). Large-scale functional analysis of the roles of phosphorylation in yeast metabolic pathways. *Sci Signal* **7**: rs6.
- Semerjian AV, Malloy DC, Poteete AR. (1989). Genetic structure of the bacteriophage P22 PL operon. *J Mol Biol* **207**: 1–13.
- Sergueev K, Yu D, Austin S, Court D. (2001). Cell toxicity caused by products of the p(L) operon of bacteriophage lambda. *Gene* **272**: 227–235.
- Shannon P, Markiel A, Ozier O, Baliga NS, Wang JT, Ramage D *et al*. (2003). Cytoscape: a software environment for integrated models of biomolecular interaction networks. *Genome Res* **13**: 2498–2504.
- Sharon I, Battchikova N, Aro E-M, Giglione C, Meinel T, Glaser F *et al*. (2011). Comparative metagenomics of microbial traits within oceanic viral communities. *ISME J* **5**: 1178–1190.
- Stover CK, Pham XQ, Erwin AL, Mizoguchi SD, Warrener P, Hickey MJ *et al*. (2000). Complete genome sequence of *Pseudomonas aeruginosa* PAO1, an opportunistic pathogen. *Nature* **406**: 959–964.
- Sullivan MB, Huang KH, Ignacio-Espinoza JC, Berlin AM, Kelly L, Weigle PR *et al*. (2010). Genomic analysis of oceanic cyanobacterial myoviruses compared with T4-like myoviruses from diverse hosts and environments. *Environ Microbiol* **12**: 3035–3056.
- Suttle CA. (2005). Viruses in the sea. *Nature* **437**: 356–361.
- Tan Y, Zhang K, Rao X, Jin X, Huang J, Zhu J *et al*. (2007). Whole genome sequencing of a novel temperate bacteriophage of *P. aeruginosa*: evidence of tRNA gene mediating integration of the phage genome into the host bacterial chromosome. *Cell Microbiol* **9**: 479–491.
- Thompson LR, Zeng Q, Kelly L, Huang KH, Singer AU, Stubbe J *et al*. (2011). Phage auxiliary metabolic genes and the redirection of cyanobacterial host carbon metabolism. *Proc Natl Acad Sci USA* **108**: E757–E764.
- Timischl B, Dettmer K, Kaspar H, Thieme M, Oefner PJ. (2008). Development of a quantitative, validated capillary electrophoresis-time of flight-mass spectrometry method with integrated high-confidence analyte identification for metabolomics. *Electrophoresis* **29**: 2203–2214.
- Traxler MF, Summers SM, Nguyen H-T, Zacharia VM, Hightower GA, Smith JT *et al*. (2008). The global, ppGpp-mediated stringent response to amino acid starvation in *Escherichia coli*. *Mol Microbiol* **68**: 1128–1148.
- Ueno H, Yonesaki T. (2004). Phage-induced change in the stability of mRNAs. *Virology* **329**: 134–141.
- Wagemans J, Blasdel BG, Van den Bossche A, Uytterhoeven B, De Smet J, Paeshuyse J *et al*. (2014). Functional elucidation of antibacterial phage ORFs targeting *Pseudomonas aeruginosa*. *Cell Microbiol* **16**: 1822–1835.
- Waggoner BT, Sultana K, Symonds N, Karlok MA, Pato ML. (1989). Identification of the bacteriophage Mu kil gene. *Virology* **173**: 378–389.
- Wang P, Selvadurai K, Huang RH. (2015). Reconstitution and structure of a bacterial Pnkp1-Rnl-Hen1 RNA repair complex. *Nat Commun* **6**: 6876.
- Weitz JS, Stock CA, Wilhelm SW, Bourouiba L, Coleman ML, Buchan A *et al*. (2015). A multitrophic model to quantify the effects of marine viruses on microbial food webs and ecosystem processes. *ISME J* **9**: 1352–1364.
- Westman EL, McNally DJ, Charchoglyan A, Brewer D, Field RA, Lam JS. (2009). Characterization of WbpB, WbpE, and WbpD and reconstitution of a pathway for the biosynthesis of UDP-2,3-diacetamido-2,3-dideoxy-D-mannuronic acid in *Pseudomonas aeruginosa*. *J Biol Chem* **284**: 11854–11862.

Supplementary Information accompanies this paper on The ISME Journal website (<http://www.nature.com/ismej>)